Ubiquitin ligase Rad18^{Sc} localizes to the XY body and to other chromosomal regions that are unpaired and transcriptionally silenced during male meiotic prophase

Roald van der Laan[1,2], Evert-Jan Uringa[2], Evelyne Wassenaar[2], Jos W. Hoogerbrugge[2], Esther Sleddens[2], Hanny Odijk[1], Henk P. Roest[1], Peter de Boer[3], Jan H. J. Hoeijmakers[1], J. Anton Grootegoed[2] and Willy M. Baarends[2,*]

[1]MGC-Department of Cell Biology and Genetics, Center for Biomedical Genetics, and [2]Department of Reproduction and Development, Erasmus MC, University Medical Center, PO Box 1738, 3000 DR Rotterdam, The Netherlands
[3]Department of Obstetrics and Gynecology, University Medical Center St Radboud, PO Box 9101, 6500 HB Nijmegen, The Netherlands
*Author for correspondence (e-mail: w.baarends@erasmusmc.nl)

Accepted 16 June 2004
Journal of Cell Science 117, 5023-5033 Published by The Company of Biologists 2004
doi:10.1242/jcs.01368

Summary

In replicative damage bypass (RDB) in yeast, the ubiquitin-conjugating enzyme RAD6 interacts with the ubiquitin ligase RAD18. In the mouse, these enzymes are represented by two homologs of RAD6, HR6a and HR6b, and one homolog of RAD18, Rad18^{Sc}. Expression of these genes and the encoded proteins is ubiquitous, but there is relatively high expression in the testis. We have studied the subcellular localization by immunostaining Rad18^{Sc} and other RDB proteins in mouse primary spermatocytes passing through meiotic prophase in spermatogenesis. The highest Rad18^{Sc} protein level is found at pachytene and diplotene, and the protein localizes mainly to the XY body, a subnuclear region that contains the transcriptionally inactivated X and Y chromosomes. In spermatocytes that carry translocations for chromosomes 1 and 13, Rad18^{Sc} protein concentrates on translocation bivalents that are not fully synapsed. The partly synapsed bivalents are often localized in the vicinity of the XY body, and show a very low level of RNA polymerase II, indicating that the chromatin is in a silent configuration similar to transcriptional silencing of the XY body. Thus, Rad18^{Sc} localizes to unsynapsed and silenced chromosome segments during the male meiotic prophase. All known functions of RAD18 in yeast are related to RDB. However, in contrast to Rad18^{Sc}, expression of UBC13 and polη, known to be involved in subsequent steps of RDB, appears to be diminished in the XY body and regions containing the unpaired translocation bivalents. Taken together, these observations suggest that the observed subnuclear localization of Rad18^{Sc} may involve a function outside the context of RDB. This function is probably related to a mechanism that signals the presence of unsynapsed chromosomal regions and subsequently leads to transcriptional silencing of these regions during male meiotic prophase.

Key words: Replicative damage bypass, Ubiquitination, Rad18^{Sc}, HR6a, HR6b, Meiosis, XY body

Introduction

Maintenance of stability of the genome of an organism is essential for proper cell function. In the germ line, genome surveillance mechanisms are essential to allow faithful transmission of genetic information to subsequent generations. Life would not be possible without various DNA damage response and repair pathways that are active in somatic and germ line cells to cope with DNA damage. We are interested in the possible gametogenic functions of proteins involved in a mechanism that tolerates the presence of DNA lesions during replication, termed replicative damage bypass (RDB, previously described as post-replication repair).

Genes involved in RDB in the yeast *Saccharomyces cerevisiae* encode members of the RAD6 epistasis group, and homologs in higher eukaryotes have been identified. Our laboratory has identified two mouse homologs of the ubiquitin-conjugating enzyme RAD6, *HR6a/Ube2a* and *HR6b/Ube2b* (Roest et al., 1996; Kwon et al., 2001), and recently we also cloned *Rad18^{Sc}*, the mouse homolog of the ubiquitin ligase *RAD18* (van der Laan et al., 2000). The *Rad18^{Sc}* gene is ubiquitously expressed in mouse tissues, but the highest level of mRNA expression is found in testis (van der Laan et al., 2000). To obtain insight into possible spermatogenic aspects of RDB and about Rad18^{Sc} functions in particular, we have analyzed the expression of Rad18^{Sc} during spermatogenesis using different mouse models.

RDB pathways are thought to be initiated by the RAD6-RAD18 protein complex, and two major downstream subpathways for RDB have been proposed: translesion synthesis (TLS) and damage avoidance (DA) (Baynton and Fuchs, 2000). Translesion synthesis is capable of bypassing a DNA lesion that blocks the replicative polymerase, by using the activity of several specialized enzymes to prevent irreversible termination of DNA replication (Friedberg and

Gerlach, 1999). These TLS polymerases include RAD30A (polη), RAD30B (polι), REV3-REV7 (polζ) and REV1 (Woodgate, 1999). Translesion synthesis polymerases take over from the replicative DNA polymerase when a given lesion is encountered, and are capable of bypassing the lesion with the incorporation of a few nucleotides. Subsequently, the activity of the replicative polymerase is reinitiated. In contrast to TLS, the DA mechanisms remain largely hypothetical. The term 'damage avoidance' refers to the fact that, in this subpathway, replication proceeds but use of the damaged DNA strand is avoided. Instead, the lesion is bypassed using homology from the newly replicated strand, or the homologous chromosome (Baynton and Fuchs, 2000). Initiation of DA subpathways requires activity of the UBC13-MMS2-RAD5 complex (Broomfield et al., 1998).

The yeast *RAD6* gene encodes an ubiquitin-conjugating enzyme (E2 enzyme). The ubiquitin system marks target proteins with one or multiple ubiquitin moieties (mono- or poly-ubiquitination) through a multi-enzyme mechanism: ubiquitin-activating enzyme E1, ubiquitin-conjugating enzyme E2 and ubiquitin ligase E3. Ubiquitinated substrates are targeted for degradation by the proteasome or they may undergo functional alterations (Pickart, 2004). It appears that RAD6 has several functions outside the context of RDB, including an involvement in sporulation, gene silencing and chromatin modification (Dover et al., 2002; Lawrence, 1994; Singh et al., 1998; Sun and Allis, 2002; Sun and Hampsey, 1999).

The deletion of both *HR6a* and *HR6b* in mice is an embryonic lethal condition (Roest et al., 2004) and even double-knockout ES cells are not obtained (H.P.R., unpublished). However, inactivation of the *HR6b* gene alone has no overall effect on development and viability of the mice, and at the cellular level no increased sensitivity for DNA damage was observed, but males were found to be infertile due to derailment of spermatogenesis (Roest et al., 1996). Mice that are HR6a-deficient also do not display a pronounced somatic phenotype, but we observed maternal factor infertility, manifested as a two-cell block of embryonic development (Roest et al., 2004). The absence of a somatic phenotype in the *HR6a* or *HR6b* single knockout animals is probably due to functional redundancy of the two RAD6 homologs in somatic cells. On the basis of these and other observations, the mammalian homologs *HR6a* and *HR6b* are thought to function in conserved aspects of RDB and also in several other processes including chromatin structure regulation (Roest et al., 1996; Baarends et al., 1999; Baarends et al., 2003; Roest, 2004). Recently, Rad18^{Sc}-deficient ES cells were generated, and these cells are defective in RDB as visualized by an increased sensitivity to various DNA damaging agents, including UV-C light, MMS, mitomycin C and cisplatin, but not to X-rays (Tateishi et al., 2003).

High expression of *Rad18^{Sc}* mRNA has been detected in primary spermatocytes, in the prophase of the first meiotic division (van der Laan et al., 2000). Following DNA replication in preleptotene spermatocytes, which is the spermatogenic final round of DNA replication, the relatively long meiotic prophase I can be subdivided into four phases: leptotene, zygotene, pachytene and diplotene. During leptotene, the chromosomes are stretched out, meiotic double-strand DNA breaks are induced, telomere clustering initiates homologous chromosome synapsis during zygotene, and axial elements are formed along the chromosomes. At pachytene, the axial elements have become lateral elements when the autosomal bivalents display complete synapsis. Synapsed chromosomes are held together as a tripartite structure, the synaptonemal complex (SC), which is composed of lateral element proteins (Sycp2 and Sycp3) and central element proteins (Sycp1 and a 48 kDa protein) (Heyting, 1996). During pachytene, crossing-overs are established that become visible as chiasmata, when disassembly of the SC starts in diplotene. Finally, the cells reach diakinesis, the stage of transition to metaphase. In meiotic prophase, the sex chromosomes are stably synapsed only along the pseudo-autosomal regions (PARs), and they form a subnuclear region called XY body (or sex body), which is first seen around early pachytene and persists into diplotene. During early pachytene, transcription from the X and Y chromosomes is globally repressed (Monesi, 1965), but following completion of the meiotic divisions several X and Y chromosomal genes are re-expressed in haploid spermatids (Hendriksen et al., 1995).

In the present study we analyzed the expression of Rad18^{Sc} protein in mouse testis in detail, and the results provide indications that Rad18^{Sc} marks unsynapsed and inactive chromosomal regions in pachytene and diplotene primary spermatocytes during meiotic prophase in the male mouse.

Materials and Methods

Antibody production

Polyclonal antibodies against the Rad18^{Sc} protein were raised in rabbits using GST-fusion proteins. Different parts of the *Rad18^{Sc}* cDNA were fused to the *GST* gene (M-version: amino acid residues 192-360, and C-version: amino acid residues 428-509). These fusion proteins were purified from a 2-liter culture using a glutathione column (Sigma Chemical Co., St Louis, MO) followed by an ion exchange column (Sp-sepharose, Sigma). Purified fusion proteins were used to immunize rabbits (two animals for each fusion protein) using Freund's (Sigma) complete adjuvant for the prime and Freund's incomplete adjuvant (Sigma) for booster injections (intra cutaneous). Pre-immune serum and antisera were tested on an immunoblot of mouse total testis lysate. One antiserum against the M-version was affinity purified using the M-version fusion protein coupled to Affigel 10 (BioRad, La Jolla, CA) and used for all described experiments unless indicated otherwise (the C-version antibody was used to verify all results obtained with the affinity-purified antibody).

Antibodies against mouse UBC13 were generated at Eurogentec (Seraing, Belgium) according to their protocols. Rabbits were immunized with a mixture of two UBC13-derived peptides (C_{21}PGIKAEPDESNARY$_{34}$ and A_{114}PNPDDPLANDVAEQ$_{128}$).

Immunoblot analysis

Mouse testes were obtained from wild-type FVB mice of different age, and frozen in liquid nitrogen directly after removal from the body. Cell preparations highly enriched in spermatocytes and round spermatids were isolated from mouse testes (FVB) after collagenase and trypsin treatment, followed by sedimentation at unit gravity (StaPut procedure) and density gradient centrifugation through Percoll (Grootegoed et al., 1984).

Protein extracts were prepared by ten cycles of 10-second sonification in 0.25 M sucrose/1mM EDTA supplemented with complete protease inhibitor cocktail (Roche, Mannheim, Germany). Protein concentrations were determined using Coomassie Plus protein assay reagent (Pierce, Rockford, IL) as described by the manufacturer.

An amount of 20 μg of protein per sample was separated on 12% SDS-polyacrylamide gels and the separated proteins were transferred to nitrocellulose membranes, using the BioRad miniprotean III system and blot cells (BioRad). Membranes were stained with Ponceau S (Sigma) according to the supplier's protocol.

Rad18Sc protein was detected using the affinity purified anti-Rad18Sc antibody described above. After blocking nonspecific sites with 2.5% w/v non-fat milk in PBS with 0.1% v/v Tween20 (blotto) for 1 hour at room temperature, antibody was added at a 1:250 dilution in fresh blotto, and incubation was continued for an additional hour at room temperature. Subsequently, nonbound antibody was removed through several washes using PBS with 0.1% v/v Tween20. The second antibody, alkaline phosphatase (AP)-conjugated goat anti-rabbit (Biosource International, Camarillo, CA) was diluted 1:1000 in blotto, and incubation was for 1 hour at room temperature. After washing with PBS with 0.1% v/v Tween20 specific signal was detected by incubation with NBT/BCIP (Sigma) according to the manufacturer's manual.

In vitro transcription-translation

Rad18Sc cDNA was cloned into the pcDNA3 plasmid (Invitrogen, Carlsbad, CA) and labeled with [35S]methionine by TnT-coupled in vitro transcription-translation according to the manufacturer's protocol (Promega, Madison, WI). The product was separated on 12% polyacrylamide gels, the gels were dried and labeled protein was detected by autoradiography.

Isolation of testis tubule fragments and immunofluorescence

Mouse testes were isolated from 21-23-day-old FVB mice, and decapsulated testes were shaken (90 cycles/minute; amplitude 20 mm in a 200 ml Erlenmeyer flask) in 20 ml PBS supplemented with collagenase (100 μg/ml), hyaluronidase (60 μg/ml), glucose (5.6 mM) and DL-lactic acid (10 mM) at 32-34°C for 50 minutes. This treatment results in dissociation of testis interstitial tissue and tubules into fragments. After addition of DNAse (1 μg/ml) and trypsin (100 μg/ml) the incubation was continued for 3 more minutes to obtain smaller tubule fragments, and this tubule preparation was then washed three times with PBS containing DNAase (1 μg/ml) and fetal calf serum 2% v/v, using centrifugation at low speed to collect the tubule fragments. Finally, the tubule fragments were cultured on coverslips in DMEM-F12 supplemented with 2% v/v fetal calf serum and antibiotics at 33°C for 2-3 days.

For immunofluorescence, all steps were performed at room temperature. Cultured tubule fragments were fixed in 2% w/v paraformaldehyde for 20 minutes and were permeabilized for 10 minutes using PBS supplemented with 0.2% Triton X-100 (Sigma). Aspecific sites were masked by blocking in PBS/ 0.5% v/v BSA/0.15% v/v glycin (PBS+) for 5 minutes. Primary antibodies (anti-Rad18Sc diluted 1:100 or anti-HR6a/b recognizing HR6a and HR6b diluted 1:100, both antibodies are rabbit polyclonals) were incubated overnight in PBS+ and subsequently the excess of the first antibody was removed by three wash steps with PBS+. The specific signal was visualized by incubation with Alexa488 (diluted 1:1000) goat anti-rabbit antibodies (Molecular Probes, Eugene, OR). After removal of the antibody and subsequent washing steps, coverslips were mounted on slides using Vectashield (Vector Laboratories, Burlingame, CA). DAPI (diluted 1:5000, Sigma) was used for nuclear staining. As controls, preimmune serum was used (anti-Rad18Sc) or the first antibody was omitted during the procedure (anti-HR6a/b). In addition, on meiotic spread preparations, anti-HR6a/b accumulates on XY body chromatin, and the specificity of this reaction was confirmed using pre-incubation of the antibody with the N-terminal epitope of HR6a/b that was used to generate the antibody (not shown).

Immunohistochemistry

Mouse testes were isolated from wild-type FVB mice and fixed in phosphate-buffered formalin (30 mM NaH_2PO_4, 45 mM Na_2HPO_4, 4% v/v formaldehyde, pH 6.8) overnight at room temperature, dehydrated and embedded in paraffin. Cross-sections of 8 μm were made and mounted on 3-aminopropyltriethoxysilane-coated slides (Sigma) and dried at 37°C overnight. Slides were deparaffinized and endogenous peroxidase was blocked by incubation with 3% v/v H_2O_2 for 20 minutes. After washing in tap water, the slides were incubated for 20 minutes in a microwave oven at 1000 W in 0.01 M citric acid, pH 6.0. After cooling down to room temperature, the slides were washed with distilled water and subsequently in PBS, and nonspecific sites were blocked for 20 minutes in 0.5% w/v non-fat milk/0.5% w/v BSA in PBS. The slides were incubated overnight at room temperature with anti-Rad18Sc antibody diluted 1:100 or with anti-PCNA diluted 1:200 (Abcam, Cambridge, UK) in 10% w/v bovine serum albumin (BSA) in PBS. The slides were washed three times for 20 minutes with PBS and incubated with the second antibody (biotinylated goat anti-rabbit; or biotinylated goat anti-mouse; DAKO, Glostrup, Denmark) diluted 1:200 in PBS containing 2% v/v normal goat serum for 2 hours. The antigen-antibody complexes were visualized with avidin-biotin complex reagent (DAKO) according to the manufacturer's protocol, followed by staining using 3,3′-diaminobenzidine tetrahydrochloride (DAB) metal concentrate (Pierce) as a substrate and counterstaining with hematoxylin.

Immunostaining of meiotic nuclear spread preparations

Nuclear spread preparations of mouse spermatocytes were made according to the protocol described previously (Peters et al., 1997b). Testes from 4-5-week-old wild-type FVB mice and of T(1;13)70H/T(1;13)Wa double-heterozygous mice (de Boer et al., 1986) (Swiss random bred HsdCpb:SE) were analyzed. The slides containing meiotic nuclear spreads were washed with PBS/0.05% v/v Triton X100 extensively and nonspecific sites were blocked by incubation in PBS/0.05% v/v Triton X100/ 5% w/v nonfat milk (blocking solution) before the addition of specific antibodies. The primary antibodies (anti-Rad18Sc, rabbit polyclonal (1:100), anti-UBC13, rabbit polyclonal (1:100), anti-Sycp3, mouse monoclonal (1:2) and rabbit polyclonal (1:500) (gift from C. Heyting, Wageningen, The Netherlands), anti-polη, rabbit polyclonal (1:50) (gift from A. Lehman, Brighton, UK), anti-PCNA mouse monoclonal (1:200) (Abcam) and mouse monoclonal anti-RNA polymerase II (1:50) (8wg16, detects total RNA polymerase II; Abcam) were diluted in blocking solution and incubated overnight at room temperature. Nonbound antibodies were removed by washing in PBS and the slides were incubated with PBS/5% w/v nonfat milk/10% v/v normal goat serum for 20 minutes at room temperature. The secondary antibodies [FITC-conjugated goat anti-rabbit and TRITC-conjugated goat anti-mouse (DAKO) 1:1000] were added, and incubation was continued for 2 more hours at room temperature. Finally, after extensive washing with PBS the slides were mounted in Vectashield (Vector Laboratories) containing DAPI.

Results

Rad18Sc protein is expressed in spermatocytes and spermatids

Rad18Sc has a calculated molecular mass of 57.3 kDa. However, antibodies against Rad18Sc protein recognize a protein of approximately 80 kDa on immunoblots of mouse total testis lysate (Fig. 1A). In addition, we performed an in vitro transcription-translation assay using *Rad18Sc* cDNA. The assay yielded a prominent protein band around 80 kDa and several low intensity bands, possibly representing degradation

products (Fig. 1B). The result of the transcription-translation assay is consistent with the immunoblot. The size difference between the calculated and observed molecular mass of Rad18^{Sc} is presumably due to the fact that the tertiary structure of the Rad18^{Sc} protein is partly maintained under the denaturating conditions of gel electrophoresis. Human RAD18^{Sc} also runs as a higher molecular mass band than expected (Tateishi et al., 2000; Xin et al., 2000).

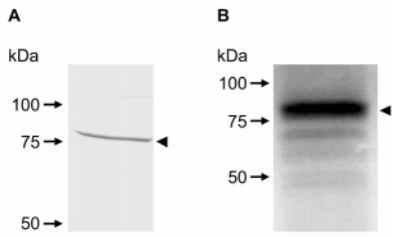

Fig. 1. Detection of Rad18^{Sc} protein. (A) On an immunoblot of proteins isolated from total testis lysate, the anti-Rad18^{Sc} antibody recognizes a specific protein band around 80 kDa (arrowhead). (B) In vitro transcription-translation using *Rad18^{Sc}* cDNA results in a protein band with a molecular mass of approximately 80 kDa (arrowhead).

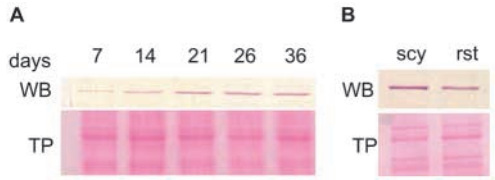

Fig. 2. Relative Rad18^{Sc} protein level in mouse testis at different postnatal developmental time points and in isolated germinal cells. (A) Total testis proteins from mice at different postnatal ages (7-36 days) were analyzed on an immunoblot (WB) using anti-Rad18^{Sc}. The relative Rad18^{Sc} protein level increases after birth to a maximum at 21 days. (B) The Rad18^{Sc} protein level in isolated spermatocytes (scy) is slightly higher than in isolated spermatids (rst). Ponceau S staining of total protein (TP) is shown as a loading control.

We performed immunoblot analysis on total testis proteins derived from wild-type FVB mice of different ages (Fig. 2A), and on proteins from isolated spermatocytes and round spermatids (Fig. 2B). In testis from 7- and 14-day-old mice the amount of Rad18^{Sc} protein is relatively low, compared with a higher level at subsequent steps of postnatal testis development. Spermatogenesis is initiated in the first week after birth, and the first wave of spermatogenesis results in population of the testis by primary spermatocytes in the period around 14 days of postnatal testis development; this is followed by the appearance of a large number of spermatids around day 21. A relatively high level of Rad18^{Sc} protein was found to be present in spermatocytes and round spermatids (Fig. 2B), which is in agreement with the observed developmental increase in Rad18^{Sc} protein level in testis (Fig. 2A).

Rad18^{Sc} protein localizes to the XY body chromatin in pachytene and diplotene spermatocytes

To study the subcellular localization of Rad18^{Sc} protein in different testicular cell types, affinity-purified polyclonal anti-Rad18^{Sc} antibody directed against amino acid residues 192-360 was used for immunohistochemical staining of mouse testis cross-sections. In addition, an antibody against the C-terminus of Rad18^{Sc} was included in the experiments to verify the results, and pre-immune sera were used as negative controls. Rad18^{Sc} protein was detected in spermatogonia, spermatocytes and round spermatids, and the highest Rad18^{Sc} protein level was found in nuclei of pachytene primary spermatocytes (Fig. 3A-C). In the nuclei of these cells, Rad18^{Sc} protein showed marked localization in a heterochromatic subnuclear region, the XY body, containing the X and Y chromosomes. When the same immunohistochemistry analysis was performed on cross-sections from a human testis biopsy, we observed a strong signal in the XY body, which probably represents high expression of RAD18^{Sc} in this subnuclear region (Fig. 3D).

In view of the interaction of RAD6-RAD18 in RDB in yeast, it is of interest to study the possible colocalization of HR6a/b and Rad18^{Sc}. The subcellular localization patterns of Rad18^{Sc} and HR6a/b proteins were compared using immunofluorescence on fixed testis tubule fragments. As both anti-Rad18^{Sc} and anti-HR6a/b were raised in rabbits, we performed the assays separately. The results indicated that the XY body chromatin in spermatocytes contains both Rad18^{Sc} and HR6a/b (Fig. 4A,B). HR6a/b protein was associated with chromatin over the whole nucleus of the primary spermatocytes in the prophase of the meiotic divisions, and it was not clear whether the XY body chromatin was highly enriched in HR6a/b.

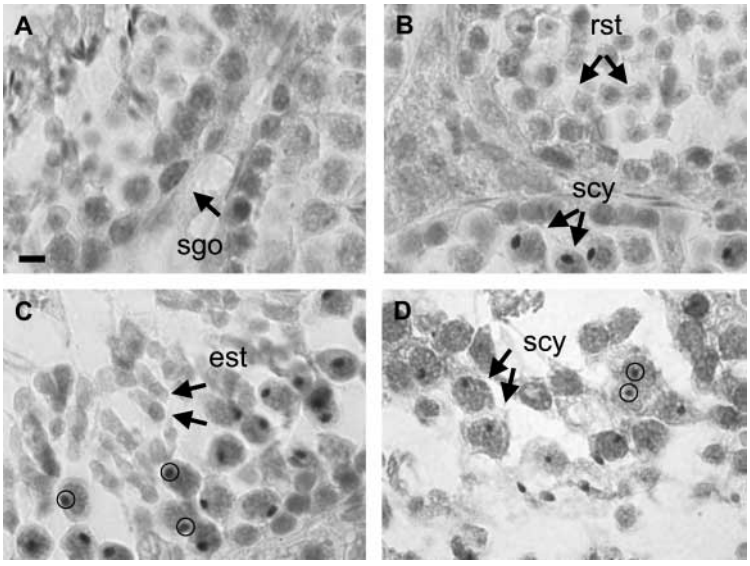

Fig. 3. Localization of Rad18^{Sc} protein in mouse and human testis. (A-C) Sections of wild-type mouse testis were stained with anti-Rad18^{Sc}. (A,B) A positive signal was found in spermatogonia (sgo), primary spermatocytes (scy) and round spermatids (rst). (C) Hardly any Rad18^{Sc} was present in elongating spermatids (est). In primary spermatocytes, the highest amount of Rad18^{Sc} was found associated with the XY body (circles). (D) In cross-sections of human testis, anti-Rad18^{Sc} gave marked staining of the XY body (circles) in primary spermatocytes (scy). Bar, 30 μm.

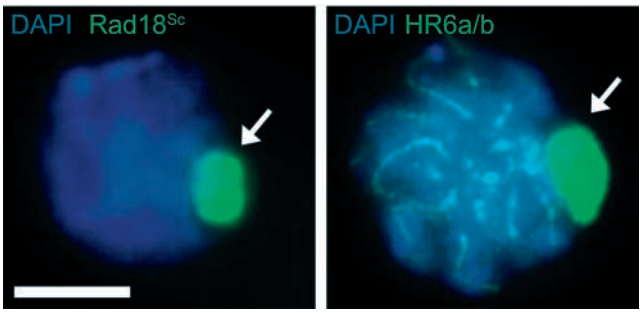

Fig. 4. Rad18Sc and HR6a/b localize to XY body chromatin in mouse primary spermatocytes. Fixed testicular tubule fragments were stained with anti-Rad18Sc (left panel) or anti-HR6a/b (right panel), and nuclei were visualized with DAPI (blue). The arrows indicate the XY body. Bar, 10 μm.

Again, a relative high level of Rad18Sc protein was limited to the XY body.

The localization of Rad18Sc to the XY body in spermatocytes was analyzed in more detail by immunostaining of meiotic spread preparations of spermatocytes, using anti-Rad18Sc antibodies in combination with an antibody against Sycp3, a major protein component of the SC. Sycp3 protein is present in the axial elements and lateral elements of the SC, and an antibody against Sycp3 can be used to mark the stages of the meiotic prophase in nuclear spread preparations of primary spermatocytes (Dobson et al., 1994; Heyting and Dietrich, 1991; Offenberg et al., 1991). HR6a/b localization was not studied because the available antibodies against HR6a/b give nonreproducible results when used for immunostaining of meiotic spread preparations.

At the zygotene stage, no clear Rad18Sc signal was visible (Fig. 5A). The XY body forms around early pachytene, and accumulation of Rad18Sc protein in the XY body was clearly visible at mid-pachytene (Fig. 5B). Rad18Sc protein localized around the XY SC and (unsynapsed) axial elements, covering the area where the X and Y chromosomes were located in the nucleus. Following further progression of the meiotic prophase, a high Rad18Sc signal was still present in the XY body in early diplotene (Fig. 5C), and thereafter the XY body and the signal disappeared (Fig. 5D).

Rad18Sc protein is present at partially synapsed translocation bivalents in spermatocytes from T(1;13)70H/T(1;13)Wa double-heterozygous mice

The marked association of Rad18Sc with XY body chromatin might be related to the fact that the large heterologous regions of the X and Y chromosomes, outside the PAR, can not undergo stable synapsis and, for the proximal Y and larger proximal part of the X, they remain unpaired throughout pachytene. To investigate whether Rad18Sc is also associated with unsynapsed autosomal regions, we used T(1;13)70H/T(1;13)Wa double-heterozygous mice (de Boer et al., 1986) in which an autosomal pairing problem occurs during spermatogenesis. This problem is caused by the presence of two different, but nearly identical, reciprocal translocations involving chromosomes 1 and 13 (de Boer et al., 1986) (Fig. 6A). The presence of the translocations leads to variable

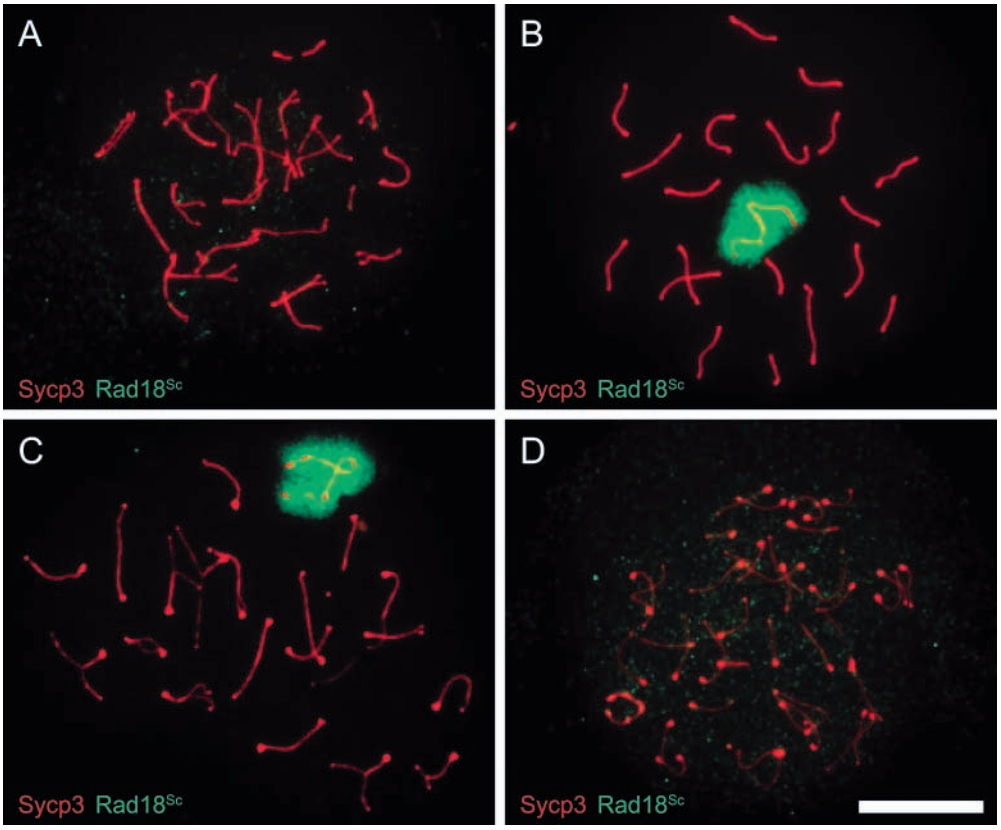

Fig. 5. Rad18Sc protein is associated with XY body chromatin of pachytene and diplotene spermatocytes. Rad18Sc is stained using anti-Rad18Sc (green) and axial elements and lateral elements of SCs are stained with anti-Sycp3 (red) in zygotene (A), pachytene (B), early diplotene (C) and diplotene (D) spermatocytes. Bar, 20 μm.

impairment of spermatogenesis, but 12-47% of the male mice generate offspring, and a sufficient number of relatively intact spermatocytes remains present, to allow the current analysis (de Boer et al., 1986; Peters et al., 1997a). During meiotic prophase, the unsynapsed axial loop of the 13^{1} translocation bivalent can be seen in early pachytene, but this loop disappears by nonhomologous synapsis in most nuclei (Moses and Poorman, 1981; Peters et al., 1997a). By contrast, resolution of the homologous 1^{13} loop is not always accomplished, and this small bivalent is often found in the vicinity of the XY body (de Boer et al., 1986; Forejt, 1996; Baart et al., 2000). In nuclear spread preparations of spermatocytes from mice with these translocations, the locations of Rad18^{Sc} and Sycp3 were visualized by immunostaining. In Fig. 6B, it is clearly visible that Rad18^{Sc} protein in pachytene spermatocytes localized not only to the XY body, but also to the 1^{13} translocation bivalent adjacent to it. However, in some nuclei the XY body accumulated Rad18^{Sc}, but the translocation bivalent did not. For the 1^{13} bivalent, different configurations of the SC have been described, associated with different degrees of homologous and/or nonhomologous synapsis (de Boer et al., 1986; Peters et al., 1997a). The morphology of the SC in primary spermatocytes from T(1;13)70H/T(1;13)Wa double-heterozygous mice, immunostained with anti-Sycp3, also shows this variability (Baart et al., 2000). To estimate the percentage pachytene nuclei with a positive Rad18^{Sc} signal on the 1^{13} bivalent, we analyzed pachytene nuclei with an overall normal SC morphology and Rad18^{Sc} signal covering the XY body. These nuclei were subdivided into four groups on the basis of different configurations of the 1^{13} bivalent: the morphology of the 1^{13} bivalent was classified according to the increasing degree of synapsis as partially synapsed rest (PR, low degree of synapsis), partially synapsed A shape (PA, intermediate degree of synapsis), partially synapsed horseshoe shape (PH, almost complete synapsis) and completely synapsed (CS). It was found that Rad18^{Sc} accumulated on the 1^{13} bivalent in almost all nuclei that contained unsynapsed 1^{13} segments (PR, PA, PH). By contrast, when synapsis of the 1^{13} bivalent was apparently complete (CS), the Rad18^{Sc} signal was very low or absent (Fig. 7). In the majority of nuclei containing the 1^{13} translocation bivalent in the PR and PA configuration, the bivalent was located in very close proximity to the XY body. By contrast, horseshoe (PH) and paired (CS) configurations of the 1^{13} bivalent were found close to the XY body in only 30% of the nuclei that carry these configurations, and Rad18^{Sc} associated with the 1^{13} bivalent in only 17.8% of the PH nuclei and not in CS nuclei. Taken together, these observations indicate that the 1^{13} bivalent loses Rad18^{Sc} protein and its tendency to colocalize with the XY body when synapsis is more complete.

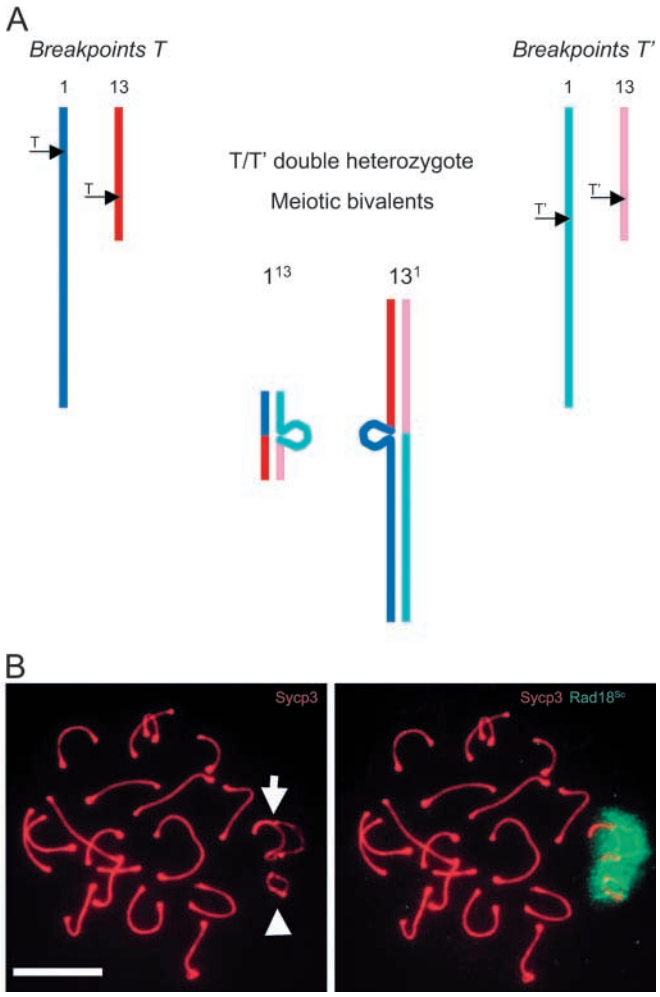

Fig. 6. Rad18^{Sc} protein localizes to unsynapsed axial loops. (A) The breakpoints (arrows) in chromosomes 1 and 13 of the T(1;13)70H (T, left) and T(1;13)Wa (T', right) mice are illustrated. Meiotic bivalents in T/T' double heterozygote mice are shown in the middle. (B) Immunostaining of Sycp3 (red) and Rad18^{Sc} (green) of T(1;13)70H/T(1;13)Wa double-heterozygous spermatocytes. Rad18^{Sc} protein localizes to the XY body and also to the translocation bivalent that shows incomplete synapsis. The unsynapsed axial loop of the 1^{13} bivalent is often found close to the XY body. The arrow indicates the X and Y bivalent (XY body) and the arrowhead points to the 1^{13} translocation bivalent. Bar, 20 μm.

XY body chromatin may not contain downstream components of RDB subpathways

In yeast, RAD6/RAD18 interaction is a key step in the activation of all RDB subpathways. Although DNA replication is completed before entry into meiotic prophase, the observed colocalization of HR6a/b and Rad18^{Sc} on XY body chromatin could signify the activation of RDB subpathways within these chromatin domains, perhaps in the context of recombination repair-associated DNA synthesis. This activation would become visible by recruitment of downstream RDB components. In yeast, one of the downstream components is UBC13. This ubiquitin-conjugating enzyme associates with MMS2 and RAD5, and together these proteins constitute a second ubiquitin-conjugating protein complex in RDB, which is thought to initiate the damage avoidance subpathway of RDB (Baynton and Fuchs, 2000; Stelter and Ulrich, 2003). The mouse homolog of *UBC13* has been identified, and the mRNA is ubiquitously expressed, but with the highest level in testis (Ashley et al., 2002). After selection of candidate antigenic peptides, a polyclonal antibody against mouse UBC13 was generated, and affinity purified. The antibody specifically recognized GST-fused mouse UBC13 on immunoblots (results not shown). Using meiotic nuclear spread preparations, UBC13 was detected in nuclei of pachytene and

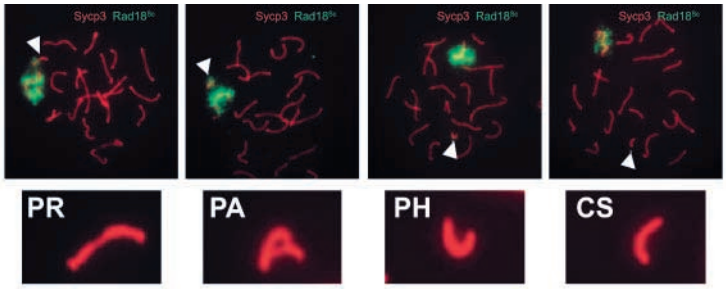

Rad18Sc signal	PR	PA	PH	CS	Tot
-	0	2	4	7	13
+/-	1	5	6	0	12
+	13	10	3	0	26
Tot	14	17	13	7	51

Fig. 7. Rad18Sc protein localizes to unsynapsed regions of the 1^{13} bivalent. The morphology of the 1^{13} bivalent was classified as partially synapsed A shape (PA, intermediate degree of synapsis), partially synapsed horsheshoe shape (PH, almost complete synapsis), partially synapsed rest (PR, low degree of synapsis), and completely synapsed (CS). The accumulation of Rad18Sc to these regions was analyzed by immunostaining (upper panel). Over groups, the number of nuclei positive for Rad18Sc was found to be increased when synapsis of these bivalents was less complete (lower panel). The arrowhead indicates the 1^{13} bivalent.

diplotene spermatocytes, and UBC13 protein was also found in postmeiotic spermatids. However, UBC13 was largely or completely excluded from XY body chromatin (Fig. 8A). On the basis of this observation, we suggest that the Rad18Sc protein does not take part in a protein complex that triggers the RDB damage avoidance subpathway in XY body chromatin. To test whether Rad18Sc in the XY body might be involved in the activation of the translesion synthesis subpathway of RDB, we used an antibody against polη, one of the TLS polymerases. The antibody used in this immunostaining is known to recognize human polη, but the peptide sequence used to generate this polyclonal antibody is 100% conserved between mouse and human (Kannouche et al., 2001). Similar to what was observed for UBC13, the amount of polη was much lower in the area of the XY body chromatin compared with the rest of the chromatin in the nuclear spread preparation (Fig. 8B), and this was not observed using pre-immune serum (result not shown). As RDB is associated with DNA replication, we also studied PCNA localization in the testis. Using immunostaining of mouse testis cross-sections and meiotic nuclear spread preparations, we did not detect PCNA in late pachytene and diplotene nuclei (results not shown). Taken together, the present results indicate that HR6a/b and Rad18Sc are associated with XY body chromatin, where they may perform some function outside the context of RDB.

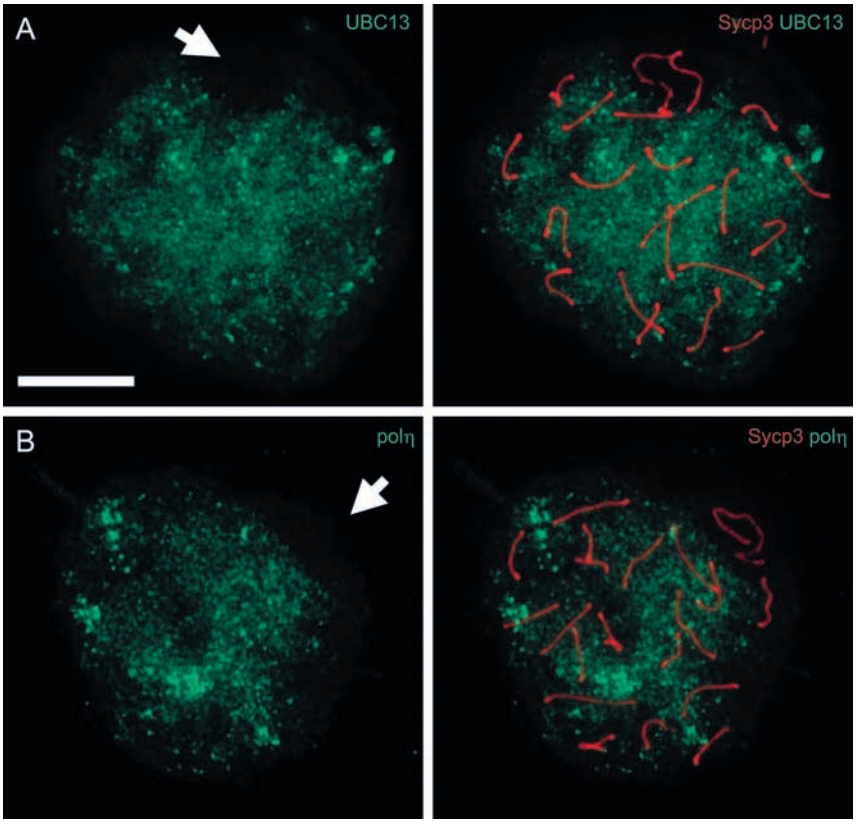

Fig. 8. Immunoexpression of RDB proteins downstream of HR6a/b-Rad18Sc is low in XY body chromatin of primary spermatocytes. (A) Left: Immunostaining of UBC13 using α-UBC13 (green) shows that UBC13 is absent from a subnuclear region where the XY body is situated (arrow). Right: Co-immunostaining of UBC13 and Sycp3 (red) to visualize the autosomes and the location of the XY body. (B) Left: Immunostaining of the TLS polymerase polη by anti-polη (green). The level of this RDB protein is also very low in the subnuclear region where the sex chromosomes are located (arrow). Right: Co-immunostaining of polη and Sycp3 (red) to visualize the autosomes and the location of the XY body. Bar, 20 μm.

Rad18^{Sc} is located in transcriptionally silenced chromatin

Yeast RAD6 exerts multiple functions, including key roles in RDB and N-end rule protein degradation, and it is also involved in sporulation and gene silencing, and in mitotic and meiotic recombination (Freiberg et al., 2000). XY body chromatin in spermatocytes is transcriptionally inactive (Monesi, 1965). We performed an immunostaining for RNA polymerase II (antibody 8wg16) to visualize transcriptional activity in spermatocytes. As previously shown by Richler et al. (Richler et al., 1994), the XY body was found to be negative for RNA polymerase II in nuclear spreads prepared from wild-type mouse testis (Fig. 9A). In T(1;13)70H/T(1;13)Wa spermatocytes, we observed a very low RNA polymerase II signal in the region where the unpaired 1^{13} loop was located (Fig. 9B). Costaining of RNA polymerase II and Rad18^{Sc} in these nuclear preparations indicates that RNA polymerase II is largely absent from regions where Rad18^{Sc} protein is abundant: the chromatin of the XY body and the unpaired 1^{13} translocation bivalent (Fig. 9C).

Discussion

The ubiquitin ligase RAD18, complexed with the ubiquitin-conjugating enzyme RAD6, is involved in replicative damage bypass (RDB) in *S. cerevisiae*. The yeast RAD6 protein performs multiple functions, including non-RDB functions, whereas RAD18 is thought to function in RDB only. The experiments described herein were performed to obtain insight into possible gametogenic functions of the mouse homolog of RAD18, Rad18^{Sc}. We have shown that Rad18^{Sc} protein expression is high in primary spermatocytes and we have found accumulation of Rad18^{Sc} on the XY body in the male meiotic prophase. HR6a/b immunostaining, representing the mouse homolog of the ubiquitin-conjugating enzyme RAD6, was also found to be present in the XY body. However, the proteins UBC13 and polη, which function downstream of HR6a/b and Rad18^{Sc} in RDB, are present in spermatocytes but do not localize to the XY body. Furthermore, we show that the presence of unpaired chromosomal segments in spermatocytes during pachytene results in transcriptional silencing and recruitment of Rad18^{Sc}. These data indicate that Rad18^{Sc} functions outside the context of RDB during the male meiotic prophase.

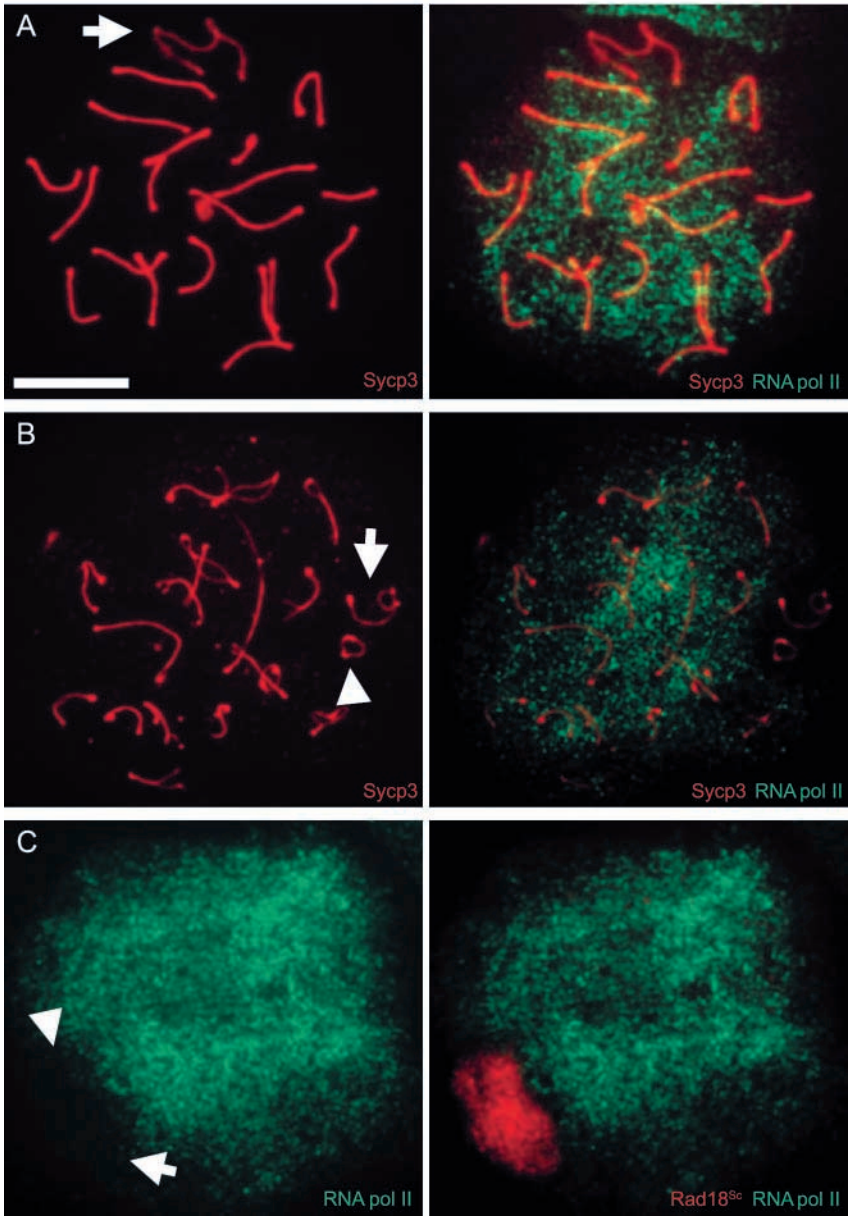

Fig. 9. RNA polymerase II is largely excluded from nuclear regions containing Rad18^{Sc} associated with unsynapsed chromosomes. (A) Left: Immunostaining of the SC using anti-Sycp3 (red) on a wild-type spermatocyte. The arrow points to the XY body. Right: Co-immunostaining of Sycp3 and RNA polymerase II (RNA pol II, green) showing that the RNA polymerase II staining signal is very low in the XY body. (B) Left: Immunostaining of Sycp3 (red) on a T(1;13)70H/T(1;13)Wa double-heterozygous spermatocyte. The arrow points to the XY body and the arrowhead to the 1^{13} translocation bivalent. Right: Co-immunostaining of Sycp3 and RNA polymerase II (RNA pol II, green) shows that the RNA polymerase II staining signal is also very low in the subnuclear region of the 1^{13} translocation bivalent. (C) Left: Immunostaining on a T(1;13)70H/T(1;13)Wa double-heterozygous spermatocyte with anti-RNA polymerase II (RNA pol II, green). The subnuclear regions containing the XY body (arrow) and the 1^{13} translocation bivalent (arrowhead) have a very low level of RNA polymerase II protein. Right: Co-immunostaining of RNA polymerase II and Rad18^{Sc} shows that the regions deficient in RNA polymerase II contain a large amount of Rad18^{Sc} (red). Bar, 20 μm.

RDB-associated Rad18Sc localization in spermatogenic cells

Immunoblot analysis of postnatal mouse testis and isolated spermatogenic cell types showed a relative high Rad18Sc protein level in primary spermatocytes, but the protein is also present in other testicular cell types, including spermatogonia, which comprise the mitotically active cell population that gives rise to new generations of spermatocytes entering meiotic prophase throughout adult reproductive life. The presence of Rad18Sc in spermatogonia might be required for RDB in these proliferating cells. The last DNA replication during spermatogenesis occurs in preleptotene primary spermatocytes, and meiotic homologous recombination during zygotene and pachytene is associated with some DNA strand elongation. This provides a possible link between DNA synthesis and high Rad18Sc expression during preleptotene and subsequent stages of meiotic prophase. However, the extreme localization of Rad18Sc to the XY body in pachytene and early diplotene is not associated with known DNA synthesis and probably serves some other function (see also below). If DNA replication occurs, PCNA should be expressed. This protein functions as a sliding clamp during DNA replication and is also required during DNA chain elongation in connection with RDB. In addition, PCNA ubiquitination occurs during RDB and depends on RAD18 in yeast and RAD18Sc in human (Hoege et al., 2002; Kannouche et al., 2004). PCNA staining has been reported for mitotically active spermatogonia and for preleptotene spermatocytes, and persistence of a low level of nuclear staining at later stages of the meiotic prophase (zygotene and early-mid pachytene) has been described (Kamel et al., 1997; Wrobel et al., 1996). In mouse testis cross-sections, using immunostaining, we did not detect PCNA in late pachytene and diplotene spermatocytes or in the XY body. Thus, RDB-associated functions of Rad18Sc during spermatogenesis are probably restricted to the S phase of spermatogonia and preleptotene spermatocytes.

The XY body, Rad18Sc and DNA repair

Apart from Rad18Sc, several other DNA repair proteins have been found to accumulate in the XY body, including Rad50, Mre11 and Ku70, all of which are involved in DNA double-strand break repair (Eijpe et al., 2000; Goedecke et al., 1999; reviewed by Hoyer-Fender, 2003). The function of these proteins with respect to the function of the XY body remains unclear. Using male mice double heterozygous for the T(1;13)70H and T(1;13)Wa translocations as described in this report, it has been shown that the XY body and the 1^{13} bivalent also stain with an antibody targeting the cell cycle checkpoint protein Atr (for ataxia telangiectasia and Rad3-related) (Keegan et al., 1996; Moens et al., 1999; Baart et al., 2000). The Atr protein is probably involved in the phosphorylation of proteins, a response of the cell cycle machinery to DNA damage (Cortez et al., 1999; Keegan et al., 1996). The intensity of Atr signal on the 1^{13} bivalent depends on the degree of pairing within this region, and the protein tends to localize to incompletely paired configurations of the bivalent (Baart et al., 2000). This protein localization pattern is similar to the present observations on Rad18Sc staining of the 1^{13} bivalent. Possibly, Atr and/or Rad18Sc also bind to unpaired chromosomal regions in oocytes that go through meiotic prophase, but this remains to be investigated. These observations suggest that localization of some proteins to the XY body is related to the presence of unsynapsed axes. In addition, XY body proteins may also have specific functions, as indicated by the existence of true XY body specific proteins (Turner et al., 2000). Possible functions of the transcriptionally inactive XY body chromatin in spermatocytes include: first, promotion and stabilization of alignment of the pseudoautosomal regions (PARs) of the X and the Y chromosomes (Turner et al., 2000); second, prevention of non-homologous recombination between regions outside the PARs of the X and Y chromosomes; and third, masking of unpaired chromosomal regions in the X and Y chromosomes from a synapsis checkpoint (Jablonka and Lamb, 1988). The only known protein that has a proven XY body function is phosphorylated histone H2AX (γ-H2AX). γ-H2AX has important roles in both DNA repair in somatic cells and meiotic recombination. Interestingly, phosphorylation of H2AX is enhanced in the XY body, and this process is essential for the formation and transcriptional silencing of the XY body (Fernandez-Capetillo et al., 2003; Mahadevaiah et al., 2001).

Rad18Sc functions in the testis outside the context of RDB

In HR6b-deficient mouse pachytene spermatocytes, we have observed lengthening of the synaptonemal complex and loss of Sycp3 from near telomeric regions (Baarends et al., 2003). Most importantly, in *HR6b* knockout spermatocytes, the number of meiotic recombination sites has increased from an average of 23, found in spermatocytes from wild-type mice, to an average of 27 (Baarends et al., 2003). This indicates that HR6b, or both HR6a and HR6b, might play some inhibitory role in the control of meiotic recombination frequency. In the XY body, such a role might implicate HR6a/b and Rad18Sc in a mechanism that acts to prevent interchromosomal meiotic recombination events outside the PARs of the X and Y chromosomes.

The present results also point to a possible function of the HR6a/b-Rad18Sc complex in a cascade of events that first signals incomplete chromosome pairing and then leads to transcriptional silencing. The XY body is transcriptionally inactive (Monesi, 1965). Using anti-RNA polymerase II antibodies, we have shown that the incompletely paired translocation 1^{13} bivalent in pachytene nuclei of male mice carrying the double-heterozygote T(1;13)70H/T(1;13)Wa translocations also becomes transcriptionally inactivated in pachytene spermatocytes. This is supported by results from early studies that have shown frequent association of different autosomal chromosomes with the XY body, when the presence of a translocation or a trisomic chromosome leads to meiotic pairing problems (Solari, 1971; de Boer and Groen, 1974; Forejt, 1974). Such XY body-associated autosomal chromosome regions are often heteropyknotic (Solari, 1971; de Boer and Groen, 1974).

RAD6 in yeast also plays a role in gene silencing, at least in part through mono-ubiquitination of histone H2B (Robzyk et al., 2000), and this function could be conserved to higher eukaryotes. By contrast, mutation of *Rad18* does not affect gene silencing, and RAD18 is not required for ubiquitination of histones. Gene function of *Rad18* in yeast is thought to be limited to RDB. Still, one report describes that yeast *rad18*

mutants combined with mutations in excision repair genes have reduced spore viability, indicating a role for RAD18 in meiosis (Dowling et al., 1985). In addition, RAD18 might be involved in the regulation of gene silencing through some other ubiquitin modification, since mutation of *chromatin assembly factor I* (*CAF1*) combined with a Δ*rad18* mutation revealed a possible role of RAD18 in telomeric silencing (Game and Kaufman, 1999). CAF1 is involved in depositing histones on DNA, and when this process is impaired, RAD6 may depend on RAD18 for recruitment to DNA (Game and Kaufman, 1999). In general, the process of inactivation of unpaired chromosomal segments might require substantial chromatin remodeling in which the HR6a/b-Rad18^{Sc} complex is involved. To further investigate the precise role of this complex, one of our next steps is to search for HR6a/b-Rad18^{Sc} substrates in spermatogenesis.

The present observations that Rad18^{Sc} localizes to unpaired and transcriptionally inactive chromosomal regions in the meiotic prophase opens a new field of interest. More detailed analysis of XY body chromatin in primary spermatocytes could give us new insights in meiotic functions of Rad18^{Sc}, and also in the mechanisms that promote formation of the XY body and control transcriptional silencing of specific chromatin domains.

We would like to thank Dr Andre Eker and Roy C. Spruijt (Rotterdam, The Netherlands) for technical assistance in the antibody production. The Sycp3 antibodies were kindly provided by Dr Christa Heyting (Wageningen, The Netherlands) and the antibodies targeting polη by Dr Alan Lehmann (Brighton, UK). This work was supported by the Dutch Cancer Foundation (EUR 99-2003).

References

Ashley, C., Pastushok, L., McKenna, S., Ellison, M. J. and Xiao, W. (2002). Roles of mouse UBC13 in DNA postreplication repair and Lys63-linked ubiquitination. *Gene* **285**, 183-191.

Baarends, W. M., Hoogerbrugge, J. W., Roest, H. P., Ooms, M., Vreeburg, J., Hoeijmakers, J. H. and Grootegoed, J. A. (1999). Histone ubiquitination and chromatin remodeling in mouse spermatogenesis. *Dev. Biol.* **207**, 322-333.

Baarends, W. M., Wassenaar, E., Hoogerbrugge, J. W., van Cappellen, G., Roest, H. P., Vreeburg, J., Ooms, M., Hoeijmakers, J. H. and Grootegoed, J. A. (2003). Loss of HR6B ubiquitin-conjugating activity results in damaged synaptonemal complex structure and increased crossing-over frequency during the male meiotic prophase. *Mol. Cell. Biol.* **23**, 1151-1162.

Baart, E. B., de Rooij, D. G., Keegan, K. S. and de Boer, P. (2000). Distribution of Atr protein in primary spermatocytes of a mouse chromosomal mutant: a comparison of preparation techniques. *Chromosoma* **109**, 139-147.

Baynton, K. and Fuchs, R. P. (2000). Lesions in DNA: hurdles for polymerases. *Trends Biochem. Sci.* **25**, 74-79.

de Boer, P. and Groen, A. (1974). Fertility and meiotic behaviour of male *T70H* tertiary trisomics of the mouse (*Mus musculus*). *Cytogenet. Cell Genet.* **13**, 489-510.

de Boer, P., Searle, A. G., van der Hoeven, F. A., de Rooij, D. G. and Beechey, C. V. (1986). Male pachytene pairing in single and double translocation heterozygotes and spermatogenic impairment in the mouse. *Chromosoma* **93**, 326-336.

Broomfield, S., Chow, B. L. and Xiao, W. (1998). MMS2, encoding a ubiquitin-conjugating-enzyme-like protein, is a member of the yeast error-free postreplication repair pathway. *Proc. Natl. Acad. Sci. USA* **95**, 5678-5683.

Cortez, D., Wang, Y., Qin, J. and Elledge, S. J. (1999). Requirement of ATM-dependent phosphorylation of brca1 in the DNA damage response to double-strand breaks. *Science* **286**, 1162-1166.

Dobson, M. J., Pearlman, R. E., Karaiskakis, A., Syropoulos, B. and Moens, P. B. (1994). Synaptonemal complex proteins: occurrence, epitope mapping and chromosome disjunction. *J. Cell Sci.* **107**, 2749-2760.

Dover, J., Schneider, J., Boateng, M. A., Wood, A., Dean, K., Johnston, M. and Shilatifard, A. (2002). Methylation of histone H3 by COMPASS requires ubiquitination of histone H2B by RAD6. *J. Biol. Chem.* **277**, 28368-28371.

Dowling, E. L., Maloney, D. H. and Fogel, S. (1985). Meiotic recombination and sporulation in repair-deficient strains of yeast. *Genetics* **109**, 283-302.

Eijpe, M., Offenberg, H., Goedecke, W. and Heyting, C. (2000). Localisation of RAD50 and MRE11 in spermatocyte nuclei of mouse and rat. *Chromosoma* **109**, 123-132.

Fernandez-Capetillo, O., Mahadevaiah, S. K., Celeste, A., Romanienko, P. J., Camerini-Otero, R. D., Bonner, W. M., Manova, K., Burgoyne, P. and Nussenzweig, A. (2003). H2AX is required for chromatin remodeling and inactivation of sex chromosomes in male mouse meiosis. *Dev. Cell* **4**, 497-508.

Forejt, J. (1974). Nonrandom association between a specific autosome and the X chromosome in meiosis of the male mouse: possible consequence of the homologous centromeres' separation. *Cytogenet. Cell Genet.* **13**, 369-383.

Forejt, J. (1996). Hybrid sterility in the mouse. *Trends Genet.* **12**, 412-417.

Freiberg, G., Mesecar, A. D., Huang, H., Hong, J. Y. and Liebman, S. W. (2000). Characterization of novel rad6/ubc2 ubiquitin-conjugating enzyme mutants in yeast. *Curr. Genet.* **37**, 221-233.

Friedberg, E. C. and Gerlach, V. L. (1999). Novel DNA polymerases offer clues to the molecular basis of mutagenesis. *Cell* **98**, 413-416.

Game, J. C. and Kaufman, P. D. (1999). Role of Saccharomyces cerevisiae chromatin assembly factor-I in repair of ultraviolet radiation damage in vivo. *Genetics* **151**, 485-497.

Goedecke, W., Eijpe, M., Offenberg, H. H., van Aalderen, M. and Heyting, C. (1999). Mre11 and Ku70 interact in somatic cells, but are differentially expressed in early meiosis. *Nat. Genet.* **23**, 194-198.

Grootegoed, J. A., Jansen, R. and van der Molen, H. J. (1984). The role of glucose, pyruvate and lactate in ATP production by rat spermatocytes and spermatids. *Biochim. Biophys. Acta* **767**, 248-256.

Hendriksen, P. J., Hoogerbrugge, J. W., Themmen, A. P., Koken, M. H., Hoeijmakers, J. H., Oostra, B. A., van der Lende, T. and Grootegoed, J. A. (1995). Postmeiotic transcription of X and Y chromosomal genes during spermatogenesis in the mouse. *Dev. Biol.* **170**, 730-733.

Heyting, C. (1996). Synaptonemal complexes: structure and function. *Curr. Opin. Cell Biol.* **8**, 389-396.

Heyting, C. and Dietrich, A. J. J. (1991). Meiotic chromosome preparation and protein labeling. *Methods Cell Biol.* **35**, 177-202.

Hoege, C., Pfander, B., Moldovan, G. L., Pyrowolakis, G. and Jentsch, S. (2002). RAD6-dependent DNA repair is linked to modification of PCNA by ubiquitin and SUMO. *Nature* **419**, 135-141.

Hoyer-Fender, S. (2003). Molecular aspects of XY body formation. *Cytogenet. Genome Res.* **103**, 245-255.

Jablonka, E. and Lamb, M. J. (1988). Meiotic pairing constraints and the activity of sex chromosomes. *J. Theor. Biol.* **133**, 23-36.

Kamel, D., Mackey, Z. B., Sjoblom, T., Walter, C. A., McCarrey, J. R., Uitto, L., Palosaari, H., Lahdetie, J., Tomkinson, A. E. and Syvaoja, J. E. (1997). Role of deoxyribonucleic acid polymerase epsilon in spermatogenesis in mice. *Biol. Reprod.* **57**, 1367-1374.

Kannouche, P., Broughton, B. C., Volker, M., Hanaoka, F., Mullenders, L. H. and Lehmann, A. R. (2001). Domain structure, localization, and function of DNA polymerase eta, defective in xeroderma pigmentosum variant cells. *Genes Dev.* **15**, 158-172.

Kannouche, P. L., Wing, J. and Lehmann, A. R. (2004). Interaction of human DNA polymerase eta with monoubiquitinated PCNA: a possible mechanism for the polymerase switch in response to DNA damage. *Mol. Cell* **14**, 491-500.

Keegan, K. S., Holtzman, D. A., Plug, A. W., Christenson, E. R., Brainerd, E. E., Flaggs, G., Bentley, N. J., Taylor, E. M., Meyn, M. S., Moss, S. B. et al. (1996). The Atr and Atm protein kinases associate with different sites along meiotically pairing chromosomes. *Genes Dev.* **10**, 2383-2388.

Kwon, Y. T., Xia, Z., Davydov, I. V., Lecker, S. H. and Varshavsky, A. (2001). Construction and analysis of mouse strains lacking the ubiquitin ligase UBR1 (E3alpha) of the N-end rule pathway. *Mol. Cell. Biol.* **21**, 8007-8021.

Lawrence, C. (1994). The *RAD6* repair pathway in *Saccharomyces cerevisiae*: what does it do, and how does it do it? *BioEssays* **16**, 253-258.

Mahadevaiah, S. K., Turner, J. M., Baudat, F., Rogakou, E. P., de Boer, P., Blanco-Rodriguez, J., Jasin, M., Keeney, S., Bonner, W. M. and

Burgoyne, P. S. (2001). Recombinational DNA double-strand breaks in mice precede synapsis. *Nat. Genet.* **27**, 271-276.

Moens, P. B., Tarsounas, M., Morita, T., Habu, T., Rottinghaus, S. T., Freire, R., Jackson, S. P., Barlow, C. and Wynshaw-Boris, A. (1999). The association of ATR protein with mouse meiotic chromosome cores. *Chromosoma* **108**, 95-102.

Monesi, V. (1965). Differential rate of ribonucleic acid synthesis in the autosomes and sex chromosomes during male meiosis in the mouse. *Chromosoma* **17**, 11-21.

Moses, M. J. and Poorman, P. A. (1981). Synaptosomal complex analysis of mouse chromosomal rearrangements. II. Synaptic adjustment in a tandem duplication. *Chromosoma* **81**, 519-535.

Offenberg, H. H., Dietrich, A. J. and Heyting, C. (1991). Tissue distribution of two major components of synaptonemal complexes of the rat. *Chromosoma* **101**, 83-91.

Peters, A. H., Plug, A. W. and de Boer, P. (1997a). Meiosis in carriers of heteromorphic bivalents: sex differences and implications for male fertility. *Chromosome Res.* **5**, 313-324.

Peters, A. H., Plug, A. W., van Vugt, M. J. and de Boer, P. (1997b). A drying-down technique for the spreading of mammalian meiocytes from the male and female germline. *Chromosome Res.* **5**, 66-68.

Pickart, C. M. (2004). Back to the future with ubiquitin. *Cell* **116**, 181-190.

Richler, C., Ast, G., Goitein, R., Wahrman, J., Sperling, R. and Sperling, J. (1994). Splicing components are excluded from the transcriptionally inactive XY body in male meiotic nuclei. *Mol. Biol. Cell* **5**, 1341-1352.

Robzyk, K., Recht, J. and Osley, M. A. (2000). Rad6-dependent ubiquitination of histone H2B in yeast. *Science* **287**, 501-504.

Roest, H. P., van Klaveren, J., de Wit, J., van Gurp, C. G., Koken, M. H., Vermey, M., van Roijen, J. H., Hoogerbrugge, J. W., Vreeburg, J. T., Baarends, W. M. et al. (1996). Inactivation of the HR6B ubiquitin-conjugating DNA repair enzyme in mice causes male sterility associated with chromatin modification. *Cell* **86**, 799-810.

Roest, H. P., Baarends, W. M., de Wit, J., van Klaveren, J. W., Wassenaar, E., Hoogerbrugge, J. W., van Cappellen, W. A., Hoeijmakers, J. H. and Grootegoed, J. A. (2004). The ubiquitin-conjugating DNA repair enzyme HR6A is a maternal factor essential for early embryonic development in mice. *Mol. Cell. Biol.* **24**, 5485-5495.

Singh, J., Goel, V. and Klar, A. J. (1998). A novel function of the DNA repair gene rhp6 in mating-type silencing by chromatin remodeling in fission yeast. *Mol. Cell. Biol.* **18**, 5511-5522.

Solari, A. J. (1971). The behaviour of chromosomal axes in Searle's X-autosome translocation. *Chromosoma* **34**, 99-112.

Stelter, P. and Ulrich, H. D. (2003). Control of spontaneous and damage-induced mutagenesis by SUMO and ubiquitin conjugation. *Nature* **425**, 188-191.

Sun, Z. W. and Allis, C. D. (2002). Ubiquitination of histone H2B regulates H3 methylation and gene silencing in yeast. *Nature* **418**, 104-108.

Sun, Z. W. and Hampsey, M. (1999). A general requirement for the Sin3-Rpd3 histone deacetylase complex in regulating silencing in Saccharomyces cerevisiae. *Genetics* **152**, 921-932.

Tateishi, S., Sakuraba, Y., Masuyama, S., Inoue, H. and Yamaizumi, M. (2000). Dysfunction of human Rad18 results in defective postreplication repair and hypersensitivity to multiple mutagens. *Proc. Natl. Acad. Sci. USA* **97**, 7927-7932.

Tateishi, S., Niwa, H., Miyazaki, J., Fujimoto, S., Inoue, H. and Yamaizumi, M. (2003). Enhanced genomic instability and defective postreplication repair in RAD18 knockout mouse embryonic stem cells. *Mol. Cell. Biol.* **23**, 474-481.

Turner, J. M., Mahadevaiah, S. K., Benavente, R., Offenberg, H. H., Heyting, C. and Burgoyne, P. S. (2000). Analysis of male meiotic "sex body" proteins during XY female meiosis provides new insights into their functions. *Chromosoma* **109**, 426-432.

van der Laan, R., Roest, H. P., Hoogerbrugge, J. W., Smit, E. M., Slater, R., Baarends, W. M., Hoeijmakers, J. H. and Grootegoed, J. A. (2000). Characterization of mRAD18Sc, a mouse homolog of the yeast postreplication repair gene RAD18. *Genomics* **69**, 86-94.

Woodgate, R. (1999). A plethora of lesion-replicating DNA polymerases. *Genes Dev.* **13**, 2191-2195.

Wrobel, K. H., Bickel, D. and Kujat, R. (1996). Immunohistochemical study of seminiferous epithelium in adult bovine testis using monoclonal antibodies against Ki-67 protein and proliferating cell nuclear antigen (PCNA). *Cell Tissue Res.* **283**, 191-201.

Xin, H., Lin, W., Sumanasekera, W., Zhang, Y., Wu, X. and Wang, Z. (2000). The human RAD18 gene product interacts with HHR6A and HHR6B. *Nucleic Acids Res.* **28**, 2847-2854.